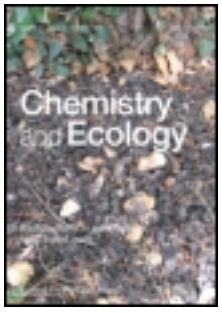

Chemistry and Ecology
Publication details, including instructions for authors and subscription information:
http://www.tandfonline.com/loi/gche20

Study of apoptosis induction using fluorescent and higher harmonic generation microscopy techniques in *Acartia tonsa* nauplii exposed to chronic concentrations of nickel

Isabella Buttino [a b], David Pellegrini [b], Giovanna Romano [a], Jiang-Shiou Hwang [c], Tzu-Ming Liu [d e], Davide Sartori [b], Chi-Kuang Sun [e f], Simona Macchia [b] & Adrianna Ianora [a]

[a] Stazione Zoologica Anton Dohrn, Naples, Italy

[b] Istituto Superiore per la Protezione e Ricerca Ambientale, ISPRA-STS, Livorno, Italy

[c] Institute of Marine Biology, National Taiwan Ocean University, Keelung, Taiwan

[d] Institute of Biomedical Engineering, National Taiwan University, Taipei, Taiwan

[e] Molecular Imaging Center, National Taiwan University, Taipei, Taiwan

[f] Department of Electrical Engineering, National Taiwan University, Taipei, Taiwan

Available online: 01 Nov 2011

Chemistry and Ecology
iFirst, 2011, 1–8

Taylor & Francis
Taylor & Francis Group

Study of apoptosis induction using fluorescent and higher harmonic generation microscopy techniques in *Acartia tonsa* nauplii exposed to chronic concentrations of nickel

Isabella Buttino[a,b]*, David Pellegrini[b], Giovanna Romano[a], Jiang-Shiou Hwang[c], Tzu-Ming Liu[d,e], Davide Sartori[b], Chi-Kuang Sun[e,f], Simona Macchia[b] and Adrianna Ianora[a]

[a]*Stazione Zoologica Anton Dohrn, Naples, Italy;* [b]*Istituto Superiore per la Protezione e Ricerca Ambientale, ISPRA-STS, Livorno, Italy;* [c]*Institute of Marine Biology, National Taiwan Ocean University, Keelung, Taiwan;* [d]*Institute of Biomedical Engineering, National Taiwan University, Taipei, Taiwan;* [e]*Molecular Imaging Center, National Taiwan University, Taipei, Taiwan;* [f]*Department of Electrical Engineering, National Taiwan University, Taipei, Taiwan*

(*Received 14 June 2011; final version recived 16 September 2011*)

In this study, we applied different fluorescent techniques to analyse the induction of apoptosis in the copepod *Acartia tonsa* nauplii exposed to low concentrations of nickel chloride ($NiCl_2$). Newly hatched and later naupliar stages were exposed to increasing concentrations of $NiCl_2$ (0.016, 0.025 and 0.063 $mg \cdot L^{-1}$) for 7 days and then stained with annexin V–FITC, a vital fluorescent probe commonly used to visualise apoptotic cells in live samples. Nauplii were also stained with TUNEL, a non-vital fluorescent probe used to detect apoptosis in fixed copepods. Moreover, we used for the first time, two-photon fluorescence (2PF) microscopy and higher harmonic generation microscopy (second SHG and third THG harmonic generation) to study apoptosis induction in *A. tonsa* nauplii without the use of fluorescent probes. 2PF and THG intensity increased in samples exposed to higher Ni concentrations, with respect to the control, whereas SHG signals were similar in all treated samples and visualised muscles. Future perspectives on the use of these new technologies to reveal apoptosis are discussed.

Keywords: confocal microscopy; two-photon fluorescence microscopy; heavy metals; ecotoxicology

1. Introduction

Apoptosis or programmed cell death is determined by precise genetic and molecular signals [1], triggered by physiological events such as metamorphosis in amphibians and fetal development in mammals, or by external factors such as exposure to toxic compounds or environmental stress [2]. Apoptotic processes induce certain peculiar characteristic events leading to morphological and biochemical alterations [3]. Among the morphological modifications are cell shrinkage, nuclear blebbing and condensation, with formation of membrane-bound vesicles called apoptotic bodies. Alteration of DNA, with consequent fragmentation and degradation, and the inversion of

*Corresponding author. Email: isabella.buttino@isprambiente.it

ISSN 0275-7540 print/ISSN 1029-0370 online

http://dx.doi.org/10.1080/02757540.2011.625944
http://www.tandfonline.com

plasma membrane permeability, coupled with the exposure of phosphatidyl serine residues to the cell surface, are other morphological events common to apoptosis in many biological systems. Moreover, specific biochemical and molecular signals, such as activation of cysteine-dependent proteases (caspases in mammals or cysteine protease homologues in non mammals) and/or release of cytochrome *c* from the mitochondrial intermembrane space to the cytosol, are part of a regulatory network consisting of pro- and anti-apoptotic factors [4]. By contrast, necrosis generally occurs when cells are exposed to extreme conditions and results in damage to the plasma membrane, with an impairment of the cell's ability to maintain homeostasis. An influx of water and extracellular ions leads to cell swelling and lysis with the release of cytoplasmic contents into the extracellular fluid. Generally, necrosis follows apoptotis in a temporal sequence depending on the intensity of the initial insult or the prevalence of one process over another [5,6]. The complexity of events inducing cellular suicide in pluricellular organisms is under continuous study, especially in humans where the characteristics of cell death are considered diagnostic.

Biochemical mechanisms of apoptosis have recently been studied in crustaceans [7], but whether apoptosis is mainly regulated, as in other arthropods (involving killer proteins as for *Drosophila melanogaster*), or rather is controlled by pro- and anti- apoptotic proteins (Bcl-2 family proteins), as occurs in vertebrates, needs to be confirmed.

From a morphological point of view, observation of cells in light microscopy, commonly used as a first screen to differentiate between apoptosis and necrosis, is not possible in crustaceans, due to the presence of a thick chitinous wall surrounding embryos, nauplii and adults. Therefore, specific fluorescent probes are the only tool to visualise apoptosis in copepods. A recent review [8] reported progress in the detection of apoptosis in marine zooplankton and described different fluorescent techniques used to visualise and differentiate apoptosis from necrosis in whole-mount copepods.

Here, we report progress in the detection of apoptosis in the marine zooplanktonic copepod *Acartia tonsa* after exposure to nickel chloride ($NiCl_2$), In addition to being ubiquitous in the biosphere and as trace element in water [9], Ni is also widely used in industry or is produced from sources such as mining, extraction and refining, and food processing. In natural waters, Ni concentrations range between 1 and 75 $\mu g \cdot L^{-1}$ [10]. It is known that Ni is toxic for humans at high concentrations, inducing nephrotoxicity, hepatotoxicity and teratogenesis [11,12], and it has been classified as carcinogenic [13]. In mammals, Ni generates reactive oxygen species [12] leading to an increase in lipid peroxidation and a loss of membrane integrity [14,15]. In aquatic environments, Ni acts as a respiratory toxicant in the cladoceran *Daphina magna* after chronic exposure [16]. Oxidative damaging effects on metallothionein synthesis have been found in the harpacticoid copepod *Tigriopus japonicus* chronically exposed to Ni [16].

With this study, we propose different microscopy techniques to identify apoptosis in copepods exposed to low concentrations of $NiCl_2$. We compare classical methods using fluorescent probes such as annexin V or TUNEL staining, with new, promising microscopy techniques such as second and third harmonic generation microscopy (SHG, THG), which can reveal apoptotic tissues in whole-mount copepods without any fluorescent probes.

2. Materials and methods

Almost 20 mature adult *A. tonsa* pairs, from a 50-L aquarium rearing tank, were sorted and incubated in a 1000 mL beaker filled with 500 mL 0.45-μm mesh net filtered seawater (Millipore 90 mm Holder YY 3009000) containing a mixture of the phytoplanktonic algae *Isochrysis galbana*, *Tetraselmis suecica* and *Rhinomonas reticulate* at a final concentration of 10^4 cells$\cdot$mL^{-1}. After 24 h, newly spawned *A. tonsa* eggs were collected from the bottom of the beaker and incubated

individually for different lengths of time (48 h, 7 days) in 2.5-mL multiwell plates containing two of these algae (*I. galbana* and *T. suecica*) provided at the above concentrations. Groups of 24 newly spawned eggs were incubated in 0.016, 0.025 and 0.063 mg·L^{-1} $NiCl_2 \times 6H_2O$ (Sigma-Aldrich, Milan, Italy). Another control group of 24 embryos was incubated in 0.45-μm filtered seawater without toxicants. Nickel solutions and food concentrations were renewed after 48 h and after 5 days.

After 7 days, the percentage of surviving nauplii was assessed. Only live nauplii were collected and incubated for 20 min with annexin V–fluorescein isothiocyanate (FITC) (Alexis Biochemicals, Switzerland) at a final concentration of 40 μl·mL^{-1}. Annexin V–FITC is a vital fluorescent probe able to bind phosphatidyl serine residues that are externalised on the plasma membrane surface during the early phases of apoptosis [17,18]. Therefore, cells undergoing apoptosis show positive green fluorescence. Nauplii were maintained in the dark and at a temperature of 20 °C and then fixed in 4% formaldehyde dissolved in seawater. They were then observed using a confocal inverted microscope Zeiss-LSM 510 with 20× to 40× objectives, and the percentage of positively stained nauplii was assessed.

Fixed nauplii were treated as reported in Buttino et al. [19] for terminal deoxynucleotidyl transferase (TdT)-mediated dUTP nick end labelling (TUNEL) staining, and observed using the confocal microscope. The same samples were also incubated with Hoechst 33342 to stain DNA, as reported in Buttino et al. [20]. For SHG and THG microscopy, 7-day-old *A. tonsa* nauplii were fixed in 4% formaldehyde for 2–4 weeks, rinsed in phosphate-buffered saline and observed with the SHG, THG and 2PF microscopy systems at the Molecular Imaging Center, National Taiwan University, Taiwan.

The nonlinear microscopy systems were excited by a home-built femtosecond Cr : forsterite laser operating around 1230 nm, which is less invasive and has deeper penetration than commonly used Ti : sapphire lasers (700–100 nm) [21,22]. The corresponding SHG and THG signals fall within the visible wavelength range, making it compatible with microscope optics. The scanned laser beam was guided to an upright microscope and focused by a 60× water immersion objective with NA = 1.2. Focusing on biological samples, the SHG contrast can reveal the distribution of structural proteins like collagens, microtubules, neurons and muscle fibres. The THG contrast can reveal the discontinuity of the refractive index by which the morphology of cells membranes, lipid vesicles, pigments and elastic fibres can be imaged. The 2PF contrast is mainly due to bilins, porphyrins, chlorophylls and their metabolites.

Because apoptosis results in apoptotic bodies enclosed by lipid membranes, such bodies can be detected by THG. Moreover, apoptosis also causes morphological abnormalities, and internal changes in copepods can be tomographically observed with SHG and THG sectioning images. These contrast mechanisms characteristic of 2PF, SHG and THG microscopy allow the imaging system to correlate intensity changes with apoptotic events.

3. Results

$NiCl_2$ was below lethal concentrations inducing 50% mortality in *A. tonsa* hatched nauplii (LC_{50}) after 48 h (0.19 to 0.25 mg·L^{-1}) and 7 days (0.038 to 0.063 mg·L^{-1}) (unpublished data). In our incubation experiments, the percentage of live nauplii after 7 days was >70% in controls, 35% in 0.025 mg·L^{-1} Ni and only 4% in 0.063 mg·L^{-1} Ni.

Figure 1 shows a 3D reconstruction of an *A. tonsa* nauplius incubated for 7 days in 0.025 mg·L^{-1} $NiCl_2$ (Figure 1a, b), and the corresponding control (Figure 1c), both of which were stained with the vital fluorescent probe annexin V–FITC and observed using the confocal laser scanning microscope. Two positively stained structures (green) are visible in the region corresponding to

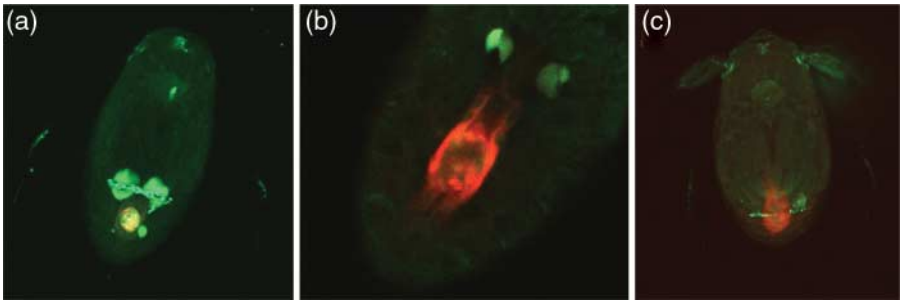

Figure 1. Three-dimensional reconstruction of *Acartia tonsa* nauplius stained with annexin V–FITC (green) and observed using a confocal laser scanning microscope. (a) Nauplius exposed to 0.025 mg·L^{-1} $NiCl_2$ for 7 days: two large structures and one small structure are positively stained with annexin (green) in the posterior part of the nauplius, while in the central and posterior part of the body, a terminal part of the digestive apparatus is stained both green and red. The red colour is due to chlorophyll autofluorescence. (b) Close-up of the posterior body of a nauplius exposed for 7 days to 0.025 mg·L^{-1} $NiCl_2$, two structures are positively stained with annexin lateral to the digestive organ which contains chlorophyll (red). (c) Control nauplius. The brightness has been increased to show diffuse and nonspecific green fluorescence. Chlorphyll (in red) is visible at the bottom of the digestive apparatus.

the beginning of the genital system (Figure 1a). A small green structure is also visible in the lower part of the body, while both red and green structures are visible in the central and posterior parts of the body. The red colour is caused by chlorophyll autofluorescence probably due to recent feeding of the animals.

Figure 1b shows a higher magnification of a nauplius incubated in 0.025 mg·L^{-1} $NiCl_2$; red fluorescence is due to chlorophyll inside the posterior digestive apparatus. Again, two structures are positively stained with annexin, laterally to the gut. Figure 1c is a control nauplius showing only the red fluorescence in the posterior part of the digestive apparatus, due to chlorophyll autofluorescence. Image brightness has been increased to highlight the very low intensity of green fluorescence. Of the live nauplii exposed to 0.025 mg·L^{-1} $NiCl_2$, >66% were positively stained with annexin V, whereas 85% showed TUNEL positivity, in contrast to controls with 30% positivity with both probes, probably due to natural apoptosis caused by imminent metamorphosis. Only 2% of nauplii exposed to 0.063 mg·L^{-1} $NiCl_2$ survived and these were not stained with TUNEL or annexin V because of the small sample size.

Fixed nauplii incubated with 0.025 mg·L^{-1} $NiCl_2$ were stained with TUNEL; when cells enter apoptosis, lysis of endonucleases triggers the cleavage of DNA into specific oligonucleosomic fragments that can be labelled on the free radical 3′OH by a fluorescent marker dUTP using TdT [23,24]. Figure 2a is a 3D reconstruction of a nauplius incubated in $NiCl_2$ and observed with three different excitation lights to visualise TUNEL (green), Hoechst (violet) and chlorophyll (red). Many nuclei appeared positively stained with TUNEL; in some areas nuclei were so bright that they covered other fluorescence (i.e. violet and red). Figure 2b is a 3D reconstruction of a control nauplius; the whole body is stained with Hoechst (violet). Green fluorescence due to TUNEL is only visible at the top of the legs, probably indicating natural apoptosis occurring during development.

Harmonic generation microscopy (HGM) is a laser scanning nonlinear microscopy technique that acquires optical sectioning images with submicron spatial resolution. The intensity of two photon red fluorescence images (Figure 3e, f, g, h) was represented with a flame-like colour scale and the fluorescence level of the control was amplified 100× to show greater detail (Figure 3e). Nauplii exposed to increasing concentrations of $NiCl_2$ (0.016, 0.025 and 0.063 mg·L^{-1}) showed an increased 2PF fluorescence in the region corresponding to the digestive apparatus (arrows in Figure 3f, g, h), compared to the control. Similarly, THG signals (M = magenta) increased in nauplii exposed to $NiCl_2$ at 0.063 mg·L^{-1}, in contrast to a weak fluorescence of control nauplii

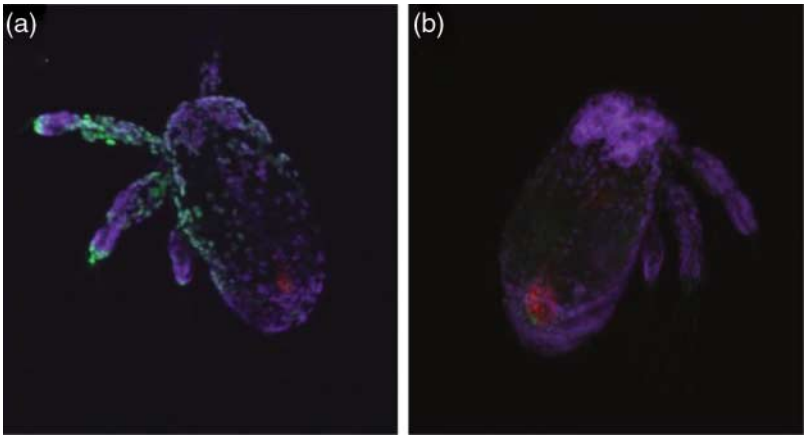

Figure 2. Three-dimensional reconstruction of *Acartia tonsa* nauplius stained with Hoechst 33342 (violet) and TUNEL (green) and observed using the confocal laser scanning microscope. (a) Nauplius exposed to 0.025 mg·L^{-1} $NiCl_2$ for 7 days was positively stained with TUNEL. Red autofluorescence is visible at the bottom of the digestive apparatus, due to chlorophyll (red). (b) Control nauplius.

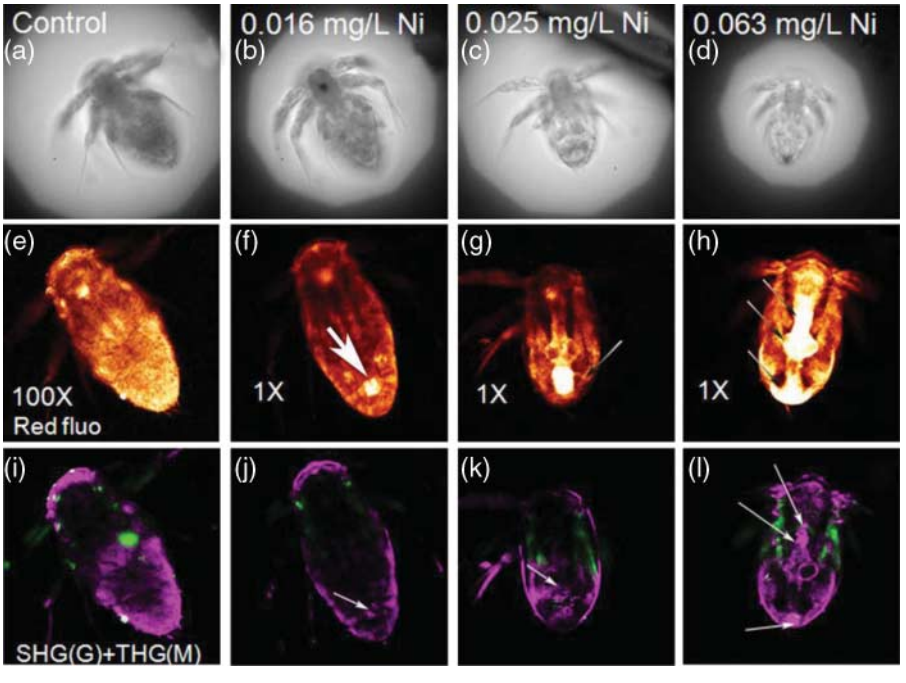

Figure 3. *Acartia tonsa* nauplius observed with light microscopy (first row), two photon fluorescence (2PF) microscopy (second row), and second (SHG) and third (THG) harmonic generation microscopy (third row). Control nauplius shows a weak autofluorescence when observed with 2PF; fluorescence output was increased 100× to visualize the structures (e). Nauplius incubated in 0.016, 0.025 and 0.063 mg·L^{-1} $NiCl_2$ for 7 days show an increased 2PF fluorescence in the region corresponding to the digestive apparatus (arrows) (f, g, h). SHG microscopy (green) shows muscles; the magenta colour represents the THG microscopy signals which increased in nauplii exposed to the highest $NiCl_2$ concentrations, in the same regions as for 2PF fluorescence (see arrows) (j, k, l). In the combined images, the strong fluorescence in nauplii exposed to 0.063 mg·L^{-1} $NiCl_2$ is evident in the inner part of the gut and in the posterior part of the body (arrows) (l).

(Figure 3i) and to those exposed to lower nickel concentrations (arrows in Figure 3j, k, l). The THG signals, evident in the inner part of the gut, could be due to the production of apoptosis-related vesicles. By contrast, SHG microscopy (G = green) revealed muscles resulting in a fluorescent signal similar to those recorded for all treatments.

4. Discussion

The use of copepods for ecotoxicological tests is not new [25]. In our study, the calanoid copepod *A. tonsa* appears to be very sensitive to Ni exposure; 0.025 $mg \cdot L^{-1}$ $NiCl_2$ strongly reduced naupliar viability to only 35% after 7 days exposure, with 85% of the surviving nauplii marked positively for apoptotis as revealed with TUNEL staining. This suggests that only 6% of the naupliar population would be recruited to adulthood in 25 $\mu g \cdot L^{-1}$ $NiCl_2$-polluted waters, a Ni concentration found in many estuaries and rivers [10].

The identification of active programmed cell death (apoptosis) in copepods is relatively new [8,26–28]. Among the classical non vital fluorescent probes used to detect apoptosis, the *in situ* nick-end labelling of DNA strand breaks (TUNEL) has been successfully used to stain copepod embryos, nauplii and adults [17,26,28]. Moreover, vital fluorescent probes such as fluorescein diacetate or its homologous Sytox green and 7-aminoactinomycin have been used to discriminate between live or dead cells in copepods. These latter stains do not differentiate between necrosis and apoptosis even though their application may be useful to rapidly detect copepod embryo viability without having to wait for eggs to hatch [18,29]. Poulet et al. [27] used a double-labelling method to stain *Calanus helgolandicus* nauplii with annexin V–FITC coupled with propidium iodide, to differentiate between apoptotic and necrotic cells in live copepod nauplii. However, use of fluorescent probes in copepods and more generally in crustaceans is difficult, due to their chitinous wall which needs to be permeabilised [8].

Our results obtained with annexin V reveal two large structures in the posterior part of the body, in the region corresponding to the gonad buds. These structures are not visible in samples stained with TUNEL, probably because of the different staining protocols. In fact, annexin V is a viable fluorescent probe and the protocol consists of the incubation of live animals in a solution. In this manner, live copepods actively ingest the probe which stains the internal organs. By contrast, the permeability of TUNEL is limited to sub-superficial body cells because the animals are fixed and then stained. Hence, the two staining methodologies (TUNEL versus annexin V) can, at times, lead to different results.

Our data obtained with non-invasive SHG and THG microscopy show that these techniques, applied in copepods for the first time, can be useful to detect apoptosis in both live and fixed copepods, without any preliminary treatment or fluorescent probes. Therefore, both techniques may represent an innovative approach to study copepod toxicology. THG microscopy can depict the boundaries of cells or the distribution of vesicles. Its signal intensity is determined by the contrast of the refractive index and a material-related constant [24,30,31]. SHG microscopy has been shown to reveal the distribution and orientation of structured proteins such as collagens or microtubules [24]. In a recent article, strong THG signals were found associated to the apoptotic bodies in the hind brain of zebrafish. The same apoptotic bodies were positively stained with acridine orange and detected by 2PF [32,33]. In our experiments 2PF increased in nauplii exposed to higher concentrations of heavy metals. The signals detected are in the same regions that are positively stained with annexin V. Moreover, THG fluorescence increased in nauplii exposed to higher concentrations of Ni, as also demonstrated in zebrafish embryos, suggesting that this method is able to visualise apoptosis induction. If this hypothesis is confirmed by further studies, this noninvasive technique can be used to predict naupliar mortality in live organisms without using any fluorescent probes.

Interestingly, the three different approaches used in this study revealed different sensitive regions: TUNEL was able to differentiate cells and their fluorescence in apopototic regions including small spots, annexin-V stained organs with a particular affinity to lipid structures, such as the gonadic buds, whereas 2PF microscopy was able to detect apoptotic tissues with a diffuse fluorescence, including the autofluorescence due to chlorophyll emission. In general, the image quality obtained using SHG and THG fluorescence microscopy was more detailed, with THG able to reveal very fine structures inside the copepod gut. Whether these signals are, in fact, due to apopototis must be further investigated, possibly using different molecular approaches.

Our preliminary results open up new and unexpected possibilities for predicting embryo and naupliar viability in zooplanktonic communities using fluorescent probes and new imaging techniques such as 2PF and THG microscopy in addition to confocal microscopy. Because some apparently normal copepod embryos or deformed nauplii are positive for apoptotic markers such as annexin and TUNEL, the possibility to predict egg, naupliar and adult mortality appears realistic and this approach should be considered in future ecotoxicology studies.

Acknowledgements

This research has partially been supported by the National Health Research Institute of Taiwan, through grant NHRI-EX98-9201EI and grant NHRI-EX100-993EI, by the National Science Council of Taiwan through grant NSC 98-2112-M-002-022; by the bilateral project SZN-NSC grant NSC 99-2923-B-019-001-MY2, and by ISPRA. Special thanks are due to Mario Di Pinto and Dr. Francesco Esposito for their support.

References

[1] G.T. Williams, *Programmed cell death: Apoptosis and oncogenesis*, Cell. 65 (1991), pp. 1097–1098.
[2] R.P. Rastogi, R. Richa, and R.P. Sinha, *Apoptosis: Molecular mechanisms and pathogenicity*, EXCLI J. 8 (2009), pp. 155–181.
[3] D.V. Krysko, T.V. Berghe, K. D'Herde, and P. Vandenabeele, *Apoptosis and necrosis: Detection, discrimination and phagocytosis*, Methods. 44 (2008), pp. 205–221.
[4] J. Yuan, S. Shaham, S. Ledoux, H.M. Ellis, and R.H. Horvitz, *The* C. elegans *cell death gene* ced-3 *encodes a protein similar to mammalian interleukin-1β-converting enzym*e, Cell. 75 (1993), pp. 641–652.
[5] E.J. Behilarz, C.E. Williams, M. Dragunow, E.S. Sirimanne, and P.D. Gluckman, *Mechanisms of delayed cell death following hypoxic–ischemic injury in the immature rat: Evidence for apoptosis during selective neuronal loss*, Mol. Brain Res. 29 (1995), pp. 1–14.
[6] M. Leist and P. Nicotera, *The shape of cell death*, Biochem. Biophys. Res. Commun. 236 (1997), pp. 1–9.
[7] M.A. Menze, G. Fortner, S. Nag, and S.C. Hang, *Mechanisms of apoptosis in Crustacea: What conditions induce versus suppress cell death?* Apoptosis 15 (2010), pp. 293–312.
[8] I. Buttino, J.-S. Hwang, C.-K. Sun, C.-T. Hsieh, T.-M. Liu, D. Pellegrini, A. Ianora, D. Sartori, G. Romano, S.-H. Cheng, and A. Miralto, *Apoptosis to predict copepod mortality: State of the art and future perspectives*, Hydrobiologia 666 (2011), pp. 257–264.
[9] S. Woo, S. Yum, H.S. Park, T.K. Lee, and J.C. Ryu, *Effects of heavy metals on atioxidatns and stress-responsive gene expression in Javanese medaka* (Oryzias javanicus), Comp. Biochem. Physiol. C 149 (2009), pp. 289–299.
[10] R. Eisler, *Nickel hazards to fish, wildilife, and invertebtrates: A synoptic review*, US Geological Survey, Biological Resources Division, Biological Science Report, 1998, pp. 1998–2001.
[11] A. Mas, D. Holt, and M. Webb, *The acute toxicity and teratogenicitiy of nickel in pregnant rats*, Toxicology 35 (1985), pp. 47–57.
[12] K. Vijayavel, S. Gopalakrishnan, R. Thiagarajan, and H. Thilagam, *Immunotoxic effects of nickel in the mud crab* Scylla serrata, Fish Shellfish Immun. 26 (2009), pp. 133–139.
[13] L.T. Haber, L. Erdreicht, G.L. Diamond, A.M. Maier, R. Ratney, Q. Zhao, and M.L. Dourson, *Hazard identification and dose response of inhaled nichel-soluble salts*, Regul. Toxicol. Pharmacol. 31 (2000), pp. 210–230.
[14] M.D. Ptashynski, R.M. Pedlar, R.E. Evans, K.G. Wautier, C.B. Baron, and J.F. Klaverkamp, *Accumulation, distribution, and toxicology of dietary nickel in lake whitefish* (Coregonus clupeaformis) *and lake trout* (Salvelinus namaycush), Comp. Biochem. Physiol. C 130 (2001), pp. 145–162.
[15] M.D. Ptashynski, R.M. Pedlar, R.E. Evans, C.B. Baron, and J.F. Klaverkamp, *Toxicology of dietary nickel in lake whitefish* (Coregonus clupeaformis), Aquat. Toxicol. 58 (2002), pp. 229–247.
[16] E.F. Pane, C. Smith, J. McGeer, and C.M. Wood, *Mechanisms of acute and chronic waterborne nickel toxicity in the freshwater cladoceran,* Daphnia magna, Environ. Sci. Technol. 37 (2003), pp. 4382–4389.

[17] J.P. Aubry, A. Blaeckem, S. Lecoanet-Henchoz, P. Jeannin, N. Herbault, G. Caron, V. Moine, and J.Y. Bonnefoy, *Annexin-V used for measuring apoptosis in the early events of cellular cytotoxicity*, Cytometry 37 (1999), pp. 197–204.
[18] E. Bossy-Wetzel and D.R. Green, *Detection of apoptosis by annexin V labeling*, in *Methods in Enzymology*, J.C. Reed, ed., Academic Press, San Diego, 2000, pp. 15–18.
[19] I. Buttino, G. De Rosa, Y. Carotenuto, M. Mazzela, A. Ianora, F. Esposito, V. Vitiello, F. Quaglia, M.I. La Rotonda, and A. Miralto, *Aldehyde-encapsulating liposomes impair marine grazer survivorship*, J. Exp. Biol. 211 (2008), 1426–1433.
[20] I. Buttino, A. Ianora, Y. Carotenuto, and A. Miralto, *Use of the confocal laser scanning microscope in studies on the developmental biology of marine crustaceans*, Microsc. Res. Tech. 60 (2003), pp. 458–464.
[21] I.-H. Chen, T.-M. Liu, P.-C. Cheng, C.-K. Sun, and B.-L. Lin, *Multimodal nonlinear spectral microscopy based on a femtosecond Cr:forsterite laser*, Opt. Lett. 26 (2001), pp. 1909–1911.
[22] C.-K Sun, S.-W. Chu, S.-Y. Chen, T.-H. Tsai, T.-M. Liu, C-H. Lin, and H.-J. Tsai, *Higher harmonic generation microscopy for developmental biology*, J. Struct. Biol. 147 (2004), pp. 19–30.
[23] S. Iseki and T. Mori, *Histochemical detection of DNA strand scissions in mammalian cells by in situ nick translation*, Cell Biol. Int. Report 9 (1985), pp. 471–477.
[24] S.H. Kaufmann, P.W. Mesner, K. Samejima, S. Toné, and W.C. Earnshaw, *Detection of DNA cleavage in apoptotic cells*, in *Methods in Enzymology, Apoptosis*, J.C. Reed, ed., Academic press, San Diego, 2000, pp. 3–11.
[25] S. Raisuddin, K.W.H. Kwok, K.M.Y. Leung, D. Schlenk, and J-S Lee, *The copepod* Tigriopus*: a promising marine model organism for ecotoxicology and environmental genomics*, Aquat. Toxicol. 83 (2007), pp. 161–173.
[26] G. Romano, G.L. Russo, I. Buttino, A. Ianora, and A. Miralto, *A marine diatom derived aldehyde induces apoptosis in copepod and sea urchin embryos*, J. Exp. Biol. 206 (2003), pp. 3487–3494.
[27] S.A Poulet, M. Richer de Forges, A. Cueff, and J.F. Lennon, *Double-labelling methods used to diagnose apoptotic and necrotic cell degradations in copepod nauplii*, Mar. Biol. 143 (2003), pp. 889–895.
[28] A. Ianora, A. Miralto, S.A. Poulet, Y. Carotenuto, I. Buttino, G. Romano, R. Casotti, G. Pohnert, T. Wichard, L. Colucci-D'Amato, G. Terrazzano, and V. Smetacek, *Aldehyde suppression of copepod recruitment in blooms of a ubiquitous planktonic diatom*, Nature 429 (2004), pp. 403–407.
[29] I. Buttino, M. do Espirito Santo, A. Ianora, and A. Miralto, *Rapid assessment of copepod embryo viability using fluorescent probes*, Mar. Biol. 145 (2004), pp. 393–399.
[30] S.-W. Chu, S.-Y. Chen, T.-H. Tsai and T.-M. Liu, C.-Y. Lin, H.-J. Tsai, and C.-K. Sun, *In vivo developmental biology study using non invasive multi-harmonic generation microscopy*, Opt. Expr. 11 (2003), pp. 3093–3099.
[31] T.-M. Liu, Y.-W. Lee, C.-F. Chang, S.-C. Yeh, C.-H. Wang, S.-W. Chu, and C.-K. Sun, *Imaging polyhedral inclusion bodies of nuclear polyhedrosis viruses with second harmonic generation microscopy*, Opt. Expr. 16 (2008), pp. 5602–5608.
[32] S.-Y. Chen, C.-S. Hsieh, S.-W. Chu, C.-H. Lin, C.-Y. Ko, Y.- C. Chen, H.-J. Tsai, C.-H. Hu, and C.-K. Sun, *Noninvasive harmonics optical microscopy for long-term observation of embryonic nervous system development in vivo*, J. Biomed. Opt. 11 (2006), pp. 054022 1–8.
[33] C.-S. Hsieh, C.-Y. Ko, S.-Y. Chen, T.-M. Liu, J.-S. Wu, C.-H. Hu, and C.-K. Sun, *In vivo long-term continuous observation of gene expression in zebrafish embryo nerve systems by using harmonic generation microscopy and morphant technology*, J. Biomed. Opt. 13 (2008), pp. 064041 1-7.